STRUCTURAL AND OPTICAL PROPERTIES OF COMPOSITES CONTAINING $A^{III}B^{VI}$ AND $A^{II}B^{VI}$ SEMICONDUCTORS

Igor Evtodiev[1,2], Dumitru Untila[1,2], Silvia Evtodiev[1], Iuliana Caraman[3], Petru Gasin [1], Liliana Dmitroglo[1], Irina Rotaru [1], and Valeriu Kantser[1,2]

[1]Moldova State University, A. Mateevici 60, Chisinau, MD-2009 Republic of Moldova;
[2]Ghitu Institute of Electronic Engineering and Nanotechnologies, Academy of Sciences of Moldova, Academiei 3/3, Chisinau, MD-2028 Republic of Moldova;
[3]Vasile Alecsandri University of Bacau, Calea Marasesti 157, Bacau, 600115 Romania
E-mail: dumitru.untila@yahoo.com

(Received June 14, 2017)

Abstract

By thermal annealing of InSe, GaSe, and GaTe crystals in Zn vapors at 800, 870, and 1050K, respectively, a material consisting of ZnSe crystallites in both GaSe and InSe and ZnTe in GaTe has been prepared. Structural defects induced by intercalated atoms shield excitonic bonds in primary compounds and form both radiative recombination levels and electron trapping levels localized deep in the band gap of $A^{III}B^{VI}$ crystals. The energies of trapping levels have been determined from thermally stimulated luminescence curves.

1. Introduction

The $A^{III}B^{VI}$ layered compounds (GaS, GaSe, GaTe, and InSe) are semiconductors of high natural anisotropy determined by the layered structure formed of planar packings of B–A–A–B type [1, 2]. These materials have the band gap in a wide energy range of 1.2 eV (InSe) to 2.5 eV (GaS) and reduced adsorption at the packing surface of atoms from the atmosphere. These are few properties that stimulate their intense research due to their perspective use in different optoelectronic and photoelectronic devices and ionizing radiations [3–8].

Anisotropy of the physical properties of these layered semiconductors in the single crystalline state is determined by the presence of two types of atoms bonding [9]. Strong ionic-covalent forces act between atomic planes within packings, while polarization forces act between elementary packings [10, 11]. Elementary packings have an arrangement that lead to the formation of cracks between them, which have a width sufficient for intercalation of both atoms and molecules; as a result, micro and nanocrystallites are formed [11–13]. At the same time, a surplus of dopant atoms introduced into these semiconductors to expand the range of their physical properties accumulates between the packings [14–18]. Under certain temperature conditions, the dopant and intercalant atoms form chemical bonds with chalcogen atoms from outside the planes of the elementary packings [13, 19]. At high temperatures, simultaneously with the formation of chemical bonds between the packings, materials composed of micro- and nanocrystallites of both the base compound and the chalcogenides of intercalant are formed [20–24].

In this paper, the crystalline structure and photo- and thermoluminescence of composites obtained by the thermal annealing of GaSe, GaTe, and InSe single crystals in *Zn* vapors are studied.

2. Experimental

GaSe, InSe, and GaTe single crystals used as a primary material for obtaining composites with ZnSe and ZnTe were grown by the vertical Bridgman–Stockbarger method [25]. At the initial stage, GaSe, InSe, and GaTe compounds were synthesized from elementary components Ga (5N), In (5N), Te (5N), and Se (5N) taken in stoichiometric quantities. The synthesis of ~20-g ingots was performed in quartz tubes with an internal diameter of ~12 mm, evacuated to a remnant pressure of $<5 \times 10^{-6}$ Torr. The synthesis temperature was ~50 K higher than the melting temperature of the synthesized compound (1230 K for GaSe, 1100 K for GaTe, and 933 K for InSe). After 24-h synthesis, the melt was passed through a temperature gradient of 5 K/cm at a rate of 0.3 mm/h.

Both *p*-GaSe and *p*-GaTe single crystals were obtained with a hole concentration of 2×10^{14} to 3×10^{14} cm^{-3} and 6×10^{15} to 8×10^{15} cm^{-3}, respectively, at the chamber temperature. The obtained InSe single crystals were of *n* type with an electron concentration of 2×10^{15} cm^{-3} and a mobility of $\sim 6 \times 10^{2}$ $cm^2/(V\ s)$ at the chamber temperature. Due to weak bonds between the elementary packings, the GaSe and InSe single crystals cleave in a direction perpendicular to the C_6 axis. The splitting direction of the GaTe single crystals coincides with the C_2 axis of a monoclinic lattice.

For photoluminescence (PL) and thermally stimulated luminescence (TSL) measurements, plates with an area of about 0.5–1.0 cm^2 and a thickness of 50 μm to 3–4 mm were cleaved from single-crystalline ingots. To prepare composite materials, GaSe, InSe, and GaTe single-crystalline plates were introduced together with Zn metal (2 mg/cm^3) in different tubes with an internal diameter of 15–16 mm. After gas evacuation to a pressure of $\sim 5 \times 10^{-6}$ Torr, the tubes were sealed. Thermal annealing was performed at temperatures of 800, 870, and 1050 K for the InSe, GaSe, and GaTe samples, respectively. At these temperatures, the Zn vapor pressure was 10^{-1}–10^{2} Torr [26]. The treatment duration was 4–24 h. Before treatment, the samples surface, which was smooth at nanometric scale, was covered with a granular layer without any well-defined structure.

The structure and composition of the resulting material was studied by XRD method with a Rigaku Ultima IV diffractometer (CuK_α radiation, λ = 1.54060 Å, 40 kV at 40 mA; a Rigaku D/teX Ultra silicon strip detector (Japan)) in the Bragg–Brentano (θ–2θ) geometry.

PL in a temperature range of 78–293 K was excited with an Nd–YAG laser (λ = 532 nm, P = 100 mW) for GaSe and the GaSe composite and with a He–Ne laser (λ = 632.8 nm, P = 20 mW) for GaTe and InSe and their composites. PL spectra were recorded using a system with a MDR-2 monochromator with a 600-mm^{-1} diffraction grating at a resolution of ~1 meV.

TSL curves of the primary single crystals and the resulting composites were recorded in a continuous radiation flow mode. A photomultiplier with a multialkali photocathode was used as a photoreceptor.

3. Experimental Results and Discussion

The XRD pattern of the GaSe single crystals thermally annealed in Zn vapors at a temperature of 870 K for 3 h is shown in Fig. 1a. It exhibits diffraction lines from the atomic planes oriented perpendicular to the C_6 crystallographic axis. The GaSe single crystals have a hexagonal lattice with parameters a = 3.7569 Å and c = 15.944 Å characteristic of the ε-polytype of GaSe (PDF 37-0931). Annealing leads to an increase in the number of free bonds in the surface layer of elementary packings and, accordingly, to an increase in structural defects, which can become

formation centers for the ZnSe compound. At a high temperature, the accumulation of dislocations occurs [27]; this process contributes to the amplification of XRD lines from the planes oriented oblique to the C_6 crystallographic axis. As can be seen from the XRD pattern, the composite obtained by thermal annealing of GaSe in Zn vapors exhibits reflections from GaSe crystallites with Miller indexes (1 0 0), (1 0 5), (1 0 7), and (2 0 2) and from the atomic planes with Miller indexes (1 1 1), (2 2 0), (3 1 1), and (4 2 0) of ZnSe crystallites with a cubic lattice with parameter a = 5.663 Å [28]. The formation of chemical bonds by the Zn atoms intercalated in the space between the elementary packings leads to the appearance of free Ga atoms that form Ga crystallites. This assumption is confirmed by the XRD lines present at 2θ angles of 23.20°, 30.26°, 30.56°, 45.41°, and 46.38°, which, according to PDF 01-074-6392, are reflections from atomic planes of Ga crystallites. Thus, thermal annealing of gallium selenide at temperatures lower than the melting point of this material in Zn vapors leads to the formation of a composite consisting of GaSe base crystallites, ZnSe crystallites, and Ga.

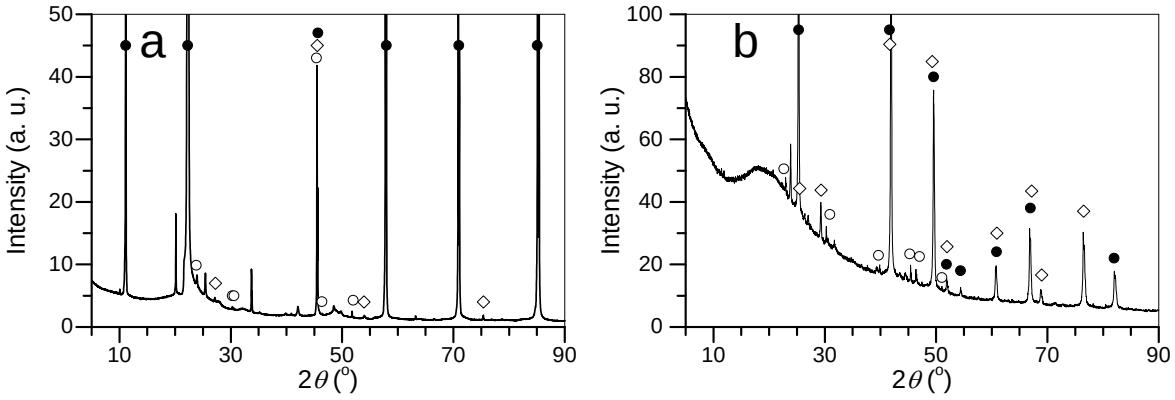

Fig. 1. XRD patterns of single crystals thermally annealed in Zn vapors: (a) GaSe, 1050 K, 3 h. ● – GaSe, PDF 37-0931; ◊ - ZnSe, PDF 70-0777; ○ - Ga, PDF 74-6392; (b) GaTe, 1070 K, 3 h. ● – GaTe, PDF 74-8974; ◊ - ZnTe, PDF 72-4848; ○ - Ga, PDF 74-6392.

Figure 1 shows the XRD pattern of the material obtained by thermal treatment of GaTe crystals in Zn vapors at 1050 K. It is evident that, in addition to XRD lines of the GaTe compound, lines from the atomic planes with Miller indexes (0 0 2), (1 0 0), (1 0 1), (1 1 0), (4 0 0), (4 2 0), and (4 2 2) characteristic of ZnTe crystallites are present. Moreover, the composite contains Ga crystallites, as determined from the presence of the lines observed in the case of the GaSe–ZnSe–Ga composite.

Figure 2 shows the PL spectra of the GaSe–ZnSe composite at 80 K. At this temperature, the PL spectrum of the pure GaSe single crystals exhibits emission lines of localized direct excitons (A_1), first LO phonon repetition (A_2), a weak emission band of indirect excitons (D), and band C determined by the radiative recombination through lattice defects [29]. Intercalation process of Zn atoms at a temperature of 870 K in the space between the elementary packings contributes to an increase in the intrinsic defect concentration in the GaSe crystallites, which efficiently shield

the excitonic bonds. The PL spectrum contour at 80 K covers a wide energy range of 1.8–2.62 eV and is well deconvoluted in four elementary curves with maxima at energies of 1.920, 2.040, 2.193, and 2.550 eV. The dominant band with maximum at an energy of 2.040 eV and a Gauss contour is analyzed in detail in [30]. The band with maximum at an energy of 1.920 eV is shifted by ~180 meV toward lower energies beside the emission band of free direct excitons and can be considered as an impurity PL. This interpretation is confirmed by the fact that a similar PL band is contained in the PL spectrum of GaSe doped with Cu [31]. The C and D bands are localized at energies higher than the band gap width of gallium monoselenide of 2.124 eV at 80 K [32]. The symmetric contour and the FWHM larger than that of excitonic emission bands indicate PL through ionized centers.

The PL spectrum of pure ZnSe crystals at 110 K contains one band with maximum at an energy of 2.77 eV and a contour slightly asymmetric toward low energies and is considered to be the emission of the acceptor bound excitons [33]. The impurity atoms and ions manifest themselves in the ZnSe crystals by the generation of impurity PL bands; e.g., Cr^+ ions form a PL band with maximum at an energy of 2.20 eV [33]. An impurity that leads to the formation of PL bands C and D can be free Ga atoms and structural defects in ZnSe crystallites present in the composite.

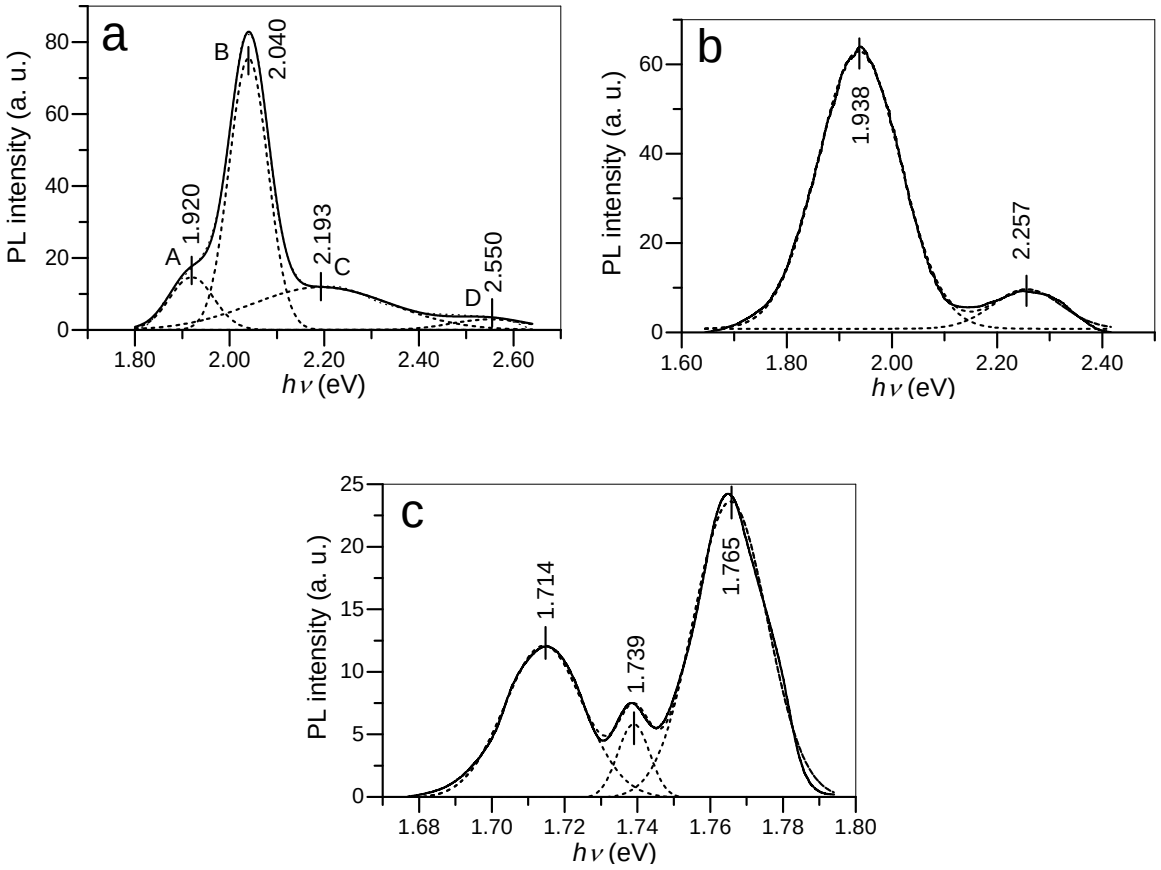

Fig. 2. PL spectra of (a) the GaSe–ZnSe, (b) InSe–ZnSe, and (c) GaTe–ZnTe composites at 80 K.

The PL spectrum of the InSe–ZnSe composite at 80 K is shown in Fig. 2b. Since the PL emission bands of InSe–ZnSe are shifted deep into the fundamental band of InSe, they can be caused by the presence of recombination levels in ZnSe crystallites present in the composite. At the chamber temperature, the PL spectrum of the composite is well described by a Gauss curve with maximum at an energy of 1.923 eV and a FWHM of ~240 meV. At 80 K, along with the dominant PL band with maximum at an energy of 1.938 eV, there is a band of lower intensity with a Gauss contour and maximum at an energy of 2.257 eV. The energetic position and the contour shape indicate the donor–acceptor nature of these two bands. The recombination levels involved in these bands are probably determined by the In surplus present in the composite.

The shape of the PL spectrum of the ZnTe–GaTe composite at a temperature of 80 K (Fig. 2c) is well described by three Gauss curves with maxima at energies of 1.764, 1.739, and 1.714 eV. The band gap width of the GaTe single crystals at 77.3 K is 1.787 eV [34]. As can be observed from Fig. 2c, the PL bands of GaTe–ZnTe are found in the region of the absorption edge of the GaTe crystallites. The maximum of the absorption band of excitons in the $n = 1$ state is found at an energy of 1.771 eV [34] and is shifted by ~7 meV toward energies higher than the maximum of the edge PL band. Thus, we can consider that the PL band with maximum at an energy of 1.764 eV represents the radiative annihilation of acceptor bound excitons with a bonding energy of 7 meV. The PL band with maximum at an energy of 1.739 eV has an analog in the PL spectrum of the pure GaTe crystals; it is determined by the lattice defects of GaTe crystals from the composite. The PL band with maximum at 1.714 eV has a Gauss contour and can be associated with the recombination mechanism through the center formed by the Zn^+ ions in the GaTe crystallites. As a result of GaTe lattice degradation determined by the presence of both ZnTe crystallites and intercalated atoms (Zn), in the band gap of the composite components (ZnTe and GaTe), both supplementary recombination levels for nonequilibrium charge carriers and electron trapping levels are formed.

The trapping levels diagram in the component crystallites of the resulting composites was studied by the TSL method. The TSL curves of the GaSe–ZnSe, InSe–ZnSe, and GaTe–ZnTe composites (Fig. 3) were analyzed by their deconvolution in Randall–Wilkins elementary curves, in which a semiconductor with one trapping level with energy E_M is considered and repeated trapping is neglected. In this approximation, the TSL curve contour is described by the formula [35]

$$I(T) = I_M \exp\left[1 + \frac{E}{kT}\frac{T - T_M}{T_M} - \frac{T^2}{T_M^2}\left(1 - \frac{T_M}{E}\right) exp\left(\frac{E}{kT}\frac{T - T_M}{T_M}\right) - \frac{2kT_M}{E}\right] \quad (1)$$

,

where I_M is the maximum intensity of emitted radiation, T_M is the temperature corresponding to the TSL peak, and E_t is the trapping level energy. The temperatures corresponding to elementary TSL curves (1) and energies of trapping levels calculated using the Urbach empirical formula $E_t = 25\ kT_M$ [36] are included in the table.

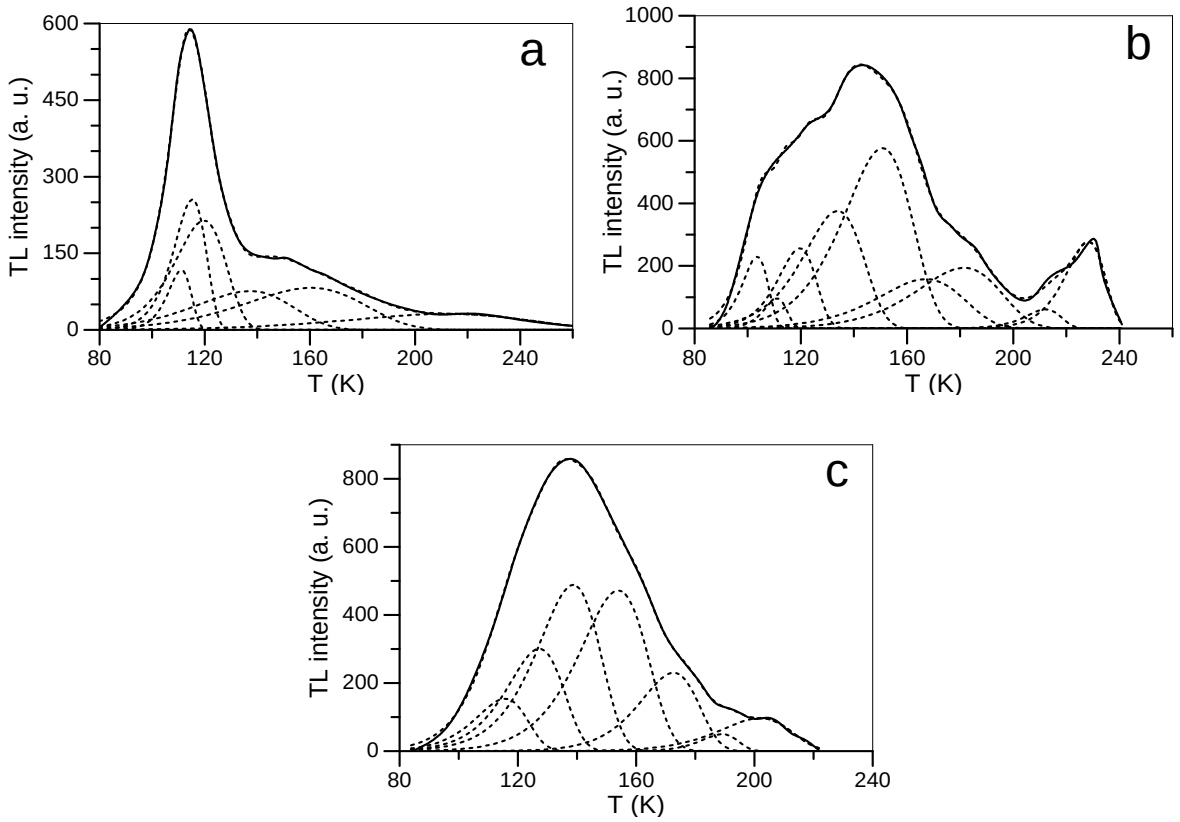

Fig. 3. TSL curves of (a) the GaSe–ZnSe, (b) InSe–ZnSe, and (c) GaTe–ZnTe composites/

Energies of trapping levels for the GaSe–ZnSe, InSe–ZnSe, and GaTe–ZnTe composites determined from TSL curves

GaSe–ZnSe		**InSe–ZnSe**		**GaTe–ZnTe**	
T_M, **K**	***E*, meV**	T_M, **K**	***E*, meV**	T_M, **K**	***E*, meV**
115	248	104	224	116	250
120	259	112	241	127	274
137	295	120	259	139	299
161	347	134	289	154	332
212	457	151	325	173	373
		167	360	189	407
		182	392	202	435
		212	457		
		228	491		

4. Conclusions

GaSe, InSe, and GaTe crystals are composed of layered packings bound by polarization forces. The Zn atoms from the vapor state intercalates in the space between the elementary

packings at 800 K for InSe, 870 K for GaSe and 1050 K for GaTe form composites consisting of InSe and ZnSe crystallites, GaSe and ZnSe crystallites, and GaTe and ZnTe crystallites, respectively. As a result of the formation of the composites, impurity levels are formed in the band gap of the primary compounds (GaSe, InSe, and GaTe) and the resulting compounds. These levels function as radiative recombination levels and electron trapping levels. The PL emission bands of the composites are formed by characteristic bands of composite components.

Acknowledgements. This work was financially supported by Moldova State University through Institutional Grant no. 15.817.02.34A. One of the authors (D. Untila) would like to thank the European Commission for financial support through Erasmus+ Programme.

References

[1] S. Pal and D.N. Bose, Sol. State Commun. 97, 725, (1996).
[2] J.F. Sanchez-Royo, A. Segura, and V. Munoz, Phys. Status Solidi A 151, 257, (1995).
[3] S. Shigetomi and T. Ikari, J. Lumin. 118, 106, (2006).
[4] F. Liu et al., ACS Nano. 8, 752, (2014).
[5] M. Reshmi et al, Int. J. Soft Comp. Engin. 1, 228, (2011).
[6] K.C. Mandal et al., IEEE Trans. Nucl. Sci. 58, 1981, (2011).
[7] Y. Hasegawa and Y. Abe, Phys. Status Solidi A. 70, 615, (1982).
[8] K. Kato and T. Mikami, Appl. Opt. 53, 2177, (2014).
[9] J.C.J.M. Terhell, Prog. Cryst. Growth Charact. Mater. 7, 55, (1983).
[10] A. Kuhn, A. Chevy, and R. Chevalier, Phys. Status Solidi A. 31, 469, (1975).
[11] S. Lei et al., Nano Lett. 13, 2777, (2013).
[12] C. Julien and M. Balkanski, Phys. Status Solidi B. 144, K147, (1987).
[13] O.A. Balitskii, B. Jaeckel, and W. Jaegermann, Phys. Lett. A. 372, 3303, (2008).
[14] W.R. McKinnon and R.R. Haering, Physical Mechanisms of Intercalation, Modern Aspects of Electrochemistry, Plenum Press, New York and London, 1983, vol. 15, chapter 4.
[15] I. Evtodiev, J. Nanoelectron. Optoelectron. 4, 76, (2009).
[16] E. Cuculescu et al., J. Optoelectron. Adv. Mater. 8, 119, (2006).
[17] V. Chiricenco et al., J. Lumin. 101, 71, (2003).
[18] S. Evtodiev et al., J. Nanoelectron. Optoelectron. 6, 502, (2011).
[19] T.M. Pekarek et al., J. Appl. Phys. 87, 6448, (2000).
[20] I. Caraman et al., Phys. Status Solidi C. 12, 70, (2015).
[21] D. Untila et al., Phys. Status Solidi C. 12, 65, (2015).
[22] N. Spalatu et al., Energy Procedia. 84, 176, (2015).
[23] I. Caraman et al., J. Optoelectron. Biomed. Mater. 7, 27, (2015).
[24] D. Untila et al., Energy Procedia 84, 149, (2015).
[25] F. Cerdeira, E.A. Meneses, and A. Gouskov, Phys. Rev. B. 16, 1648, (1977).
[26] R.E. Honig and D.A. Kramer, RCA Rev. 30, 285, (1969).
[27] S. Shigetomi, T. Ikari, and N. Nishimura, Phys. Status Solidi A. 185, 341, (2001).
[28] B.K. Agrawal, P.S. Yadav, and S. Agrawal, Phys. Rev. B: Condens. Matter. 50, 14881, (1994).
[29] L. Dmitroglo et al, Mold. J. Phys. Sci. 14, 167, (2015).
[30] M. Caraman et al., Mold. J. Phys. Sci. 14, 61, (2015).
[31] V. Capozzi and A. Minafra, J. Phys. C: Solid State Phys. 14, 4335, (1981)
[32] I. Evtodiev, J. Appl. Phys. 105, 23524, (1981).

[33] G.V. Colibaba and D.D. Nedeoglo, J. Lumin. 129, 7, 661, (2009).
[34] V.I. Gramatsky, M.I. Karaman, and V.P. Mushinsky, Fiz. Tekh. Poluprovodn. 6, 3, 550, (1972).
[35] R. Chen and Y. Kirsh, Analysis of Thermally Stimulated Processes. Pergamon Press, Oxford, New York, Toronto, Sydne, Paris,Frankfurt, 1981.
[36] V. Pagonis, G. Kitis, and C. Furetta, Numerical and Practical Exercises in Thermoluminescence. Springer Science & Business Media, 2006, 210 p.